

ARTICLE OPEN



Paternal methamphetamine exposure induces higher sensitivity to methamphetamine in male offspring through driving ADRB1 on CaMKII-positive neurons in mPFC

Yanyan Zheng^{1,2}, Dekang Liu^{1,2}, Hao Guo¹, Wenwen Chen¹, Zhaoyu Liu¹, Zhaosu Li¹, Tao Hu¹, Yuanyuan Zhang¹, Xiang Li¹, Ziheng Zhao¹, Qinglong Cai¹, Feifei Ge¹, Yu Fan¹ and Xiaowei Guan¹

© The Author(s) 2023

Paternal abuse of drugs, such as methamphetamine (METH), elevates the risk of developing addiction in subsequent generations, however, its underlying molecular mechanism remains poorly understood. Male adult mice (F0) were exposed to METH for 30 days, followed by mating with naïve female mice to create the first-generation mice (F1). When growing to adulthood, F1 were subjected to conditioned place preference (CPP) test. Subthreshold dose of METH (sd-METH), insufficient to induce CPP normally, were used in F1. Selective antagonist (betaxolol) for β_1 -adrenergic receptor (ADRB1) or its knocking-down virus were administrated into mPFC to regulate ADRB1 function and expression on CaMKII-positive neurons. METH-sired male F1 acquired sd-METH-induced CPP, indicating that paternal METH exposure induce higher sensitivity to METH in male F1. Compared with saline (SAL)-sired male F1, CaMKII-positive neuronal activity was normal without sd-METH, but strongly evoked after sd-METH treatment in METH-sired male F1 during adulthood. METH-sired male F1 had higher ADRB1 levels without sd-METH, which was kept at higher levels after sd-METH treatment in mPFC. Either inhibiting ADRB1 function with betaxolol, or knocking-down ADRB1 level on CaMKII-positive neurons (ADRB1^{CaMKII}) with virus transfection efficiently suppressed sd-METH-evoked mPFC activation, and ultimately blocked sd-METH-induced CPP in METH-sired male F1. In the process, the p-ERK1/2 and Δ FosB may be potential subsequent signals of mPFC ADRB1^{CaMKII}. The mPFC ADRB1^{CaMKII} mediates paternal METH exposure-induced higher sensitivity to drug addiction in male offspring, raising a promising pharmacological target for predicting or treating transgenerational addiction.

Translational Psychiatry (2023)13:324; <https://doi.org/10.1038/s41398-023-02624-x>

INTRODUCTION

Paternal psychostimulants intake elevates the risk of developing addiction in subsequent generations [1, 2], which remains major health concern. Methamphetamine (METH) is a commonly abused psychostimulant worldwide. One recent study found that METH-sired rats exhibit more sensitized behaviors in response to acute drug use [3], indicating that paternal METH use may enhance susceptibility to drugs in offspring. The medial prefrontal cortex (mPFC) is critically implicated in the processes of METH addiction [4, 5] and susceptibility to drugs [6–8]. Human imaging studies show that prenatal METH exposure significantly affects the volume, cortical thickness and connection of offspring brains, especially the prefrontal cortex (PFC) [7, 9, 10]. Previously, we found that mPFC were blunted to stimulants in METH-sired mice during adulthood [11]. However, the intrinsic molecular mechanism of mPFC underlying transgenerational effects of paternal METH abuse on offspring remains much to be clarified.

Adrenergic innervation on mPFC glutamatergic (CaMKII-positive) neurons plays essential roles in neurophysiology and neuropathology. The β_1 -adrenergic receptor (ADRB1) is highly expressed on mPFC CaMKII-positive neurons (ADRB1^{CaMKII}), which has been reported to participate in cognition [12, 13], reward [14],

arousal [15], motivation [16], and stress [17]. Generally, activating ADRB1 triggers neuronal excitability within PFC [18]. In animal models of cocaine-induced conditioned place preference (CPP), a model to evaluate reward and cue-related stimulations of drugs, ADRB1 administration efficiently blocks the reinstatement behaviors to cocaine in mice [19]. Prenatal events exposure, malnutrition for example, impairs the long-term potentiation in PFC of offspring, which leads to memory deficits [20–22], but could be fully recovered by ADRB1 activation [23]. These findings imply that ADRB1 might involve in drug-related transgenerational neurotoxicity, such as mPFC plasticity and vulnerability of addiction.

The β -adrenergic innervation could regulate subsequent signals through G protein-dependent or/and β -arrestin-dependent pathway. As one of classical G protein coupled receptors (GPCRs), ADRB1 has been well-studied to be coupled to Gs protein which lead to an increase in protein kinase A (PKA)-dependent signaling pathway including cAMP, PKA, and cAMP response element-binding protein (CREB) [12, 24]. Recent reports have revealed that several ligands called “biased ligands”, such as β -adrenergic receptors, elicit G protein-independent and β -arrestin-dependent pathway [25, 26], which may be served as negative feedback of the G protein-dependent pathway [27]. Huang et al. [28] found

¹Department of Human Anatomy and Histoembryology, Nanjing University of Chinese Medicine, Nanjing 210023, China. ²These authors contributed equally: Yanyan Zheng, Dekang Liu. ✉email: yfan@njucm.edu.cn; guanxw918@njucm.edu.cn

Received: 9 February 2023 Revised: 28 September 2023 Accepted: 6 October 2023

Published online: 19 October 2023

that β -Arrestin-biased β -adrenergic signaling promotes extinction learning of cocaine reward memory. At present, the price signaling pathway of ADRB1 in drug-preferred behavior remains much to be clarified.

In the present study, male adult mice (F0) were exposed to METH for 30 days, followed by mating with naïve female mice to create the first-generation mice (F1). When growing up to adult age, F1 mice were subjected to conditioned place preference (CPP) test to evaluate sensitivity to METH. Subthreshold dose of METH (sd-METH), that is insufficient to induce CPP normally, were used in F1 mice. The role of ADRB1^{CaMKII} in transgenerational susceptibility of addiction were explored in METH-sired F1 mice.

MATERIALS AND METHODS

Animals

Male C57BL/6 wild type (WT) mice weighing 22–25 g were used. All animals were housed at constant humidity (40–60%) and temperature (24 ± 2 °C) with a 12-h light/dark cycle and allowed free access to food and water. The animals were handled for three days prior to onset of experiments. All procedures were carried out in accordance with the National Institutes of Health Guide for the Care and Use of Laboratory Animals of China and approved by the Institutional Animal Care and Use Committee (IACUC) at Nanjing University of Chinese Medicine, China.

Drug treatment and tissue collection

Male C57BL/6 WT mice (F0) were assigned to administration of METH (5 mg/kg, dissolved in saline, i.p.) or saline (0.2 mL, i.p.) once daily at 10 a.m. for 30 consecutive days. At 24 h after the last injection, the F0 mice were mated with three naïve female C57BL/6 WT mice for 4 days to create METH-sired or saline-sired first-generation (F1) offspring mice.

On postnatal day 21 (PD21), male and female F1 mice were weaned and kept (4 male mice per cage) in homecage. On PD60, the mPFC tissue were collected from some male F1 mice. From PD70, some male and female F1 mice were subjected to METH-induced CPP training and test. In this study, to examine the sensitivity to METH, subthreshold dose of METH (0.25 mg/kg, sd-METH) were used to induce CPP in male F1 mice. Betaxolol, a specific β 1-adrenergic receptor (ADRB1) antagonist (Cat# S2091, Sellekchem, USA) was diluted to 0.6 μ g/ μ l in sterile saline. Brains of male F1 mice were collected on PD60 and PD73. The brains of mice on PD60 were collected without any treatment to represent baseline condition. The brains of mice on PD73 were collected within 60 min after sd-METH CPP test.

Some male naïve mice were only subjected to saline or METH treatment. On Day 1 (D1) and D2, mice were injected with saline (0.2 mL, i.p.) in the morning, and saline (0.2 mL, i.p.) or METH (0.25 mg/kg, i.p.) in the afternoon once daily at homecage. Their mPFC tissue were collected on D3 within 60 min of the last injection.

CPP

In the present study, the 0.25 mg/kg dose of METH administration, being insufficient to produce CPP in naïve mice (subthreshold dose, sd-METH), was used to induce CPP in male F1 mice and female F1 mice. The CPP test was performed in the TopScan3D CPP apparatus (CleverSys, USA), which is constructed of two distinct chambers (15 × 15 × 23 cm each) separated by a removable guillotine door. The CPP procedure consisted of three phases including the pre-conditioning test (Pre-test, PD70), conditioning (CPP training, PD71–72) and post-conditioning test (CPP test, PD73). During CPP training, both METH-sired and SAL-sired F1 mice were injected with saline (0.2 mL, i.p.) in the morning or METH (0.25 mg/kg, i.p.) in the afternoon once daily. After each injection, the mice were confined to one conditioning chamber (SAL-paired chamber or METH-paired chamber) for 45 min, and then returned to their homecage. During the Pre-test and Test, mice freely access two chambers for 15 min. The CPP score is the time spent in METH-paired chamber minus that in SAL-paired chamber, and the Δ CPP score is the CPP score of Test minus the CPP score of Pre-test.

Immunofluorescence

Briefly, the brains were perfused with 4% paraformaldehyde (PFA), and coronal brain sections (30 μ m) were cut on a cryostat (Leica, Germany). The sections were incubated in 0.3% (v/v) Triton X-100 for 0.5 h, blocked with 5% donkey serum for 1.5 h at room temperature, and incubated overnight at 4 °C with the following primary antibodies: rabbit anti-c-Fos (1:3000,

RRID:AB_2247211, Cell Signaling Technology, USA), mouse anti-NeuN (1:800, RRID:AB_2313673, Millipore, USA), mouse anti-CaMKII α (1:100, RRID:AB_626789, Santa Cruz Biotechnology, USA), mouse anti-CaMKII α (1:50, RRID:AB_2721906, Cell Signaling Technology, USA), Rabbit anti-ADRB1 (1:100, RRID:AB_10885544, Bioss, China), followed by the corresponding fluorophore-conjugated secondary antibodies for 1.5 h at room temperature. The following secondary antibodies were used here, including Alexa Fluor 555-labeled donkey anti-rabbit secondary antibody (1:500, RRID: AB_2762834, Thermo Fisher Scientific, USA), Alexa Fluor 488-labeled donkey anti-mouse secondary antibody (1:500, RRID: AB_141607, Thermo Fisher Scientific, USA). In detail of the staining for ADRB1 and NeuN, brain slices were attached to slides and placed in an oven at 60 °C for 40 min, and then immersed in 4% PFA solution for 15 min in a refrigerator at 4 °C for fixation. Then graded concentration alcohol dehydration (50%-70%-100%-100%) was performed sequentially for 5 min each time. Next, antigen repair was performed by immersing the slides with brain slices attached in 10 mM PH = 6.0 trisodium citrate solution and heating in a water bath at 82 °C for 30 min. Normal staining steps were then followed. Fluorescence signals were visualized using a Leica DM6B upright digital research microscope (Leica, Germany) and Leica TCS SP8 confocal microscope (Leica, Germany).

Western blot

Total protein was extracted from mPFC of individual mouse using RIPA lysis buffer (Beijing ComWin Biotech Co., China), Phosphatase Inhibitor (Beijing ComWin Biotech Co., China), and Protease Inhibitor (Beijing ComWin Biotech Co., China) according to the manufacturer's instructions. Protein samples (15 or 20 μ g) was separated by 10% SDS-PAGE, 12% SDS-PAGE and electrophoretically transferred onto PVDF membranes. The transferred membranes were blocked with 5% non-fat dry milk and 0.1% Tween 20 in TBST buffer for 2 h at room temperature, then subsequently incubated with the following primary antibodies: Rabbit anti-c-Fos (1:1000, RRID:AB_2247211, Cell Signaling Technology, USA), Rabbit anti-GAPDH (1:10000, RRID:AB_2651132, Bioworld Technology, USA), Rabbit anti-ADRB1 (1:1000, RRID:AB_10885544, Bioss, China), Rabbit anti-ARRB2 (1:1000, BA3767, Boster, China), Rabbit anti-ERK1/2 (1:1000, BM4326, Boster, China), Rabbit anti-phospho-ERK1/2 (1:1000, BM4156, Boster, China), Rabbit anti- Δ FosB (1:1000, bsm-52071R, Bioss, China), Rabbit anti-PKA (1:1000, bs-0520R, Bioss, China), Rabbit anti-CREB (1:1000, RRID:AB_2800317, Cell Signaling Technology, USA), Rabbit anti-phospho-CREB (1:1000, RRID:AB_2561044, Cell Signaling Technology, USA). The next day, the membranes were washed in Tris-buffered saline with Tween 20 (TBST) and incubated with horseradish peroxidase (HRP)-conjugated secondary antibody goat anti-rabbit or goat anti mouse (1:5000, Beijing ComWin Biotech Co., China) at room temperature for 1 h. The blots were visualized by the eECL Western Blot kit (Beijing ComWin Biotech Co., China, CW0049S) or ELC Kit (VazymeTM) and the signal was visualized by imaging system (Tanon-5200, China). The blots were washed with stripping buffer (Beyotime Institute of Biotechnology, China) to be reprobated with other antibodies. In this study, GAPDH was used as the loading control. The relative level of each protein expression was normalized to GAPDH. Values for target protein levels were calculated using Image J software (NIH, USA).

RNA extraction and quantitative real-time PCR

The mPFC were dissected immediately on ice. Total RNA was extracted from the mPFC using FastPure Cell/Tissue Total RNA Isolation Kit (Vazyme, China), according to the manufacturer's instructions. All samples were tested for concentration and purified using a 4200 TapeStation (Agilent Technologies, USA). After RNA extraction, the amount of RNA was normalized across samples, and cDNA was created using HiScript II Q RT SuperMix for qPCR (+gDNA wiper) (Vazyme, China). *Gapdh* was used as the internal control. The primers used in the study were as follows: *Adrb1* (forward, CTCATCGTGGTGGTAACGTG; reverse, ACACACAGCACATCTACCGAA). *c-Fos* (forward, CGGGTTTCAACGCCGACTA; reverse, TTGGCACTAGAGACGGACAGA). *Gapdh* (forward, AGGTCCGGTGTGAACGGATTTG; reverse, TGTAGACCATGTAGTTGAGGTCA). The *Adrb1* and *c-Fos* mRNA levels were normalized to *Gapdh* mRNA levels. The relative mRNA level was calculated by the comparative CT method ($2^{-\Delta\Delta C_t}$).

Local administration of betaxolol in mPFC

The cannula-double (O.D. 0.41 mm - 27 G, C.C 0.8 mm, Mates with M 3.5, Cat 62063, RWD, China) were planted into mPFC (AP + 2.7 mm, ML ± 0.4 mm, DV - 1.5 mm) of male F1 mice on PD63 before CPP training.

After surgery, mice were maintained at homecage about 1 week. From PD70, male F1 mice were subjected to sd-METH-induced CPP training. In Experiment 1 and S1, a volume of 500 nL of betaxolol (specific antagonist for ADRB1) were bilaterally injected into mPFC at a rate of 100 nL/min at 15 min prior to CPP test on PD73. In Experiment 2 and S2, a volume of 500 nL of betaxolol were bilaterally injected into the mPFC at a rate of 100 nL/min at 15 min prior to CPP training on PD71 and PD72.

Specific knockdown of ADRB1 on mPFC CaMKII-positive neurons

On PD55, mice were anesthetized with 2% isoflurane in oxygen, and were fixed in a stereotaxic frame (RWD, China). A heating pad was used to maintain the core body temperature of the mice at 36 °C. The coordinates of mPFC were defined as AP + 2.05 mm, ML ± 0.3 mm, DV - 1.9 mm. A volume of 400 nL virus of *CaMKIIap-EGFP-MIR155 (MCS)-SV40PolyA* (KD group) (Titer, 2.41 F + 13 v.g./mL; Cat, GIDV0286541, GeneChem, China) or *CaMKIIap-EGFP-SV40PolyA* (Ctrl group) (Titer, 4.01E + 12 v.g./mL; Cat, AAV9/CON540, GeneChem, China) were injected bilaterally into mPFC at a rate of 80 nL/min. After surgery, mice were kept at homecage about 3 weeks.

Dendritic spine analysis

The dendritic spines of mPFC were photographed using the z-stack scanning function of Leica TCS SP8 confocal microscope (Leica, Germany). The Spine quantification were performed under LAS X software (Leica, Germany). The number of spines were counted in the second or the third branches of dendrites from the body of CaMKII-positive neurons. Density of spines were scored in about 50 µm dendritic segments in length.

Statistical analysis

Statistical analysis was carried out using GraphPad Prism 8.0.2 software. All data are presented as the Mean ± SD. CPP score are analyzed by two-way analysis of variance (ANOVA) with Sidak's multiple comparisons test, and other data are analyzed by unpaired *t*-tests. Statistical significance was set as $P < 0.05$. All group sizes, significant differences and analyses are reported in the results section. Individual data points in the graph represent the number of experimental units (individual mouse).

RESULTS

METH-sired male F1 mice acquires sd-METH-induced CPP in adulthood

In the present study, the 0.25 mg/kg dose of METH administration (sd-METH), being insufficient to produce CPP in naïve mice (subthreshold dose), was used to induce CPP in male F1 mice (Fig. 1a) and female F1 mice (Fig. S1a).

In male F1 mice (Fig. 1b–d), sd-METH failed to induce CPP in SAL-sired male F1 ($n = 8$ mice, $t = 0.9474$, $P = 0.5872$, Fig. 1b), but increased CPP score of METH-sired male F1 ($n = 10$ mice, $t = 6.587$, $P < 0.0001$, Fig. 1b) when compared with the corresponding Pre-test data. The Δ CPP score ($t = 3.685$, $P = 0.002$, Fig. 1c) in METH-sired male F1 was higher than that in SAL-sired male F1.

In female F1 mice (Fig. S1b–d), sd-METH failed to induce CPP in both SAL-sired female F1 ($n = 8$ mice, $t = 1.398$, $P = 0.3295$, Fig. S1b) and METH-sired female F1 ($n = 10$ mice, $t = 1.979$, $P = 0.1264$, Fig. S1b) when compared with the corresponding Pre-test data. There was no significance on Δ CPP score ($t = 0.277$, $P = 0.7854$, Fig. S1c) between METH-sired female F1 and SAL-sired female F1.

These results indicate that paternal METH exposure induce higher sensitivity to METH in male, but not female offspring. As such, only male F1 mice were used to the subsequent experiments.

Sd-METH activates more CaMKII-positive neurons and induces higher ADRB1 levels in mPFC of METH-sired male F1 mice

The mPFC tissue were collected from male F1 mice on PD60 and PD73, which represent the baseline condition and responsive condition to sd-METH, respectively. The *c-Fos*, CaMKII and NeuN are used as markers to label neuronal activation, glutamatergic neuron and total neuron in mPFC, respectively.

On PD60, there was no significance in the percentage of *c-Fos*-positive & CaMKII-positive neurons in subregions of mPFC including cingulate cortex (Cg1, $t = 0.595$, $P = 0.5839$), prelimbic cortex (PrL, $t = 0.0371$, $P = 0.9722$) and infralimbic cortex (IL, $t = 0.4451$, $P = 0.6793$) between METH-sired male F1 ($n = 3$ mice) and SAL-sired male F1 ($n = 3$ mice, Fig. 1e). While on PD73 following sd-METH, the percentage of *c-Fos*-positive & CaMKII-positive neurons were at higher levels in Cg1 ($t = 3.447$, $P = 0.0137$), PrL ($t = 3.539$, $P = 0.0076$) and IL ($t = 3.160$, $P = 0.0134$) of METH-sired male F1 ($n = 4$ –5 mice) than that of SAL-sired male F1 ($n = 4$ –5 mice, Fig. 1f). On PD73, the neurons (labeled with DAPI) were more activated in Cg1 ($t = 3.031$, $P = 0.0163$), PrL ($t = 4.227$, $P = 0.0022$) and IL ($t = 4.098$, $P = 0.0027$, Fig. S2a), and the dendritic spine density of CaMKII-positive neurons was increased ($t = 4.960$, $P = 0.0026$, Fig. S2b) in mPFC of METH-sired male F1 ($n = 4$ –6 mice) than of SAL-sired male F1 ($n = 4$ –6 mice). On PD60, the baseline levels of mPFC *c-Fos* ($t = 3.496$, $P = 0.0058$) was obviously lower in METH-sired male F1 ($n = 6$ mice) than that in SAL-sired male F1 ($n = 6$ mice, Fig. 1g). On PD73 following sd-METH, there was similar levels of *c-Fos* protein ($t = 0.5061$, $P = 0.6238$) in METH-sired male F1 ($n = 6$ mice) than in SAL-sired male F1 ($n = 6$ mice, Fig. 1h). These results indicate that paternal METH exposure did not change or even reduce the mPFC activity, but obviously increased mPFC response to sd-METH, especially for CaMKII-positive neurons.

On PD60, the baseline levels of mPFC *Adrb1* gene ($t = 3.084$, $P = 0.0368$, Fig. 1i) and ADRB1 protein ($t = 2.400$, $P = 0.0373$, Fig. 1j) were higher in METH-sired male F1 (qPCR: $n = 3$ mice; protein: $n = 6$ mice) than that in SAL-sired male F1 (qPCR: $n = 3$ mice; protein: $n = 6$ mice). On PD73 following sd-METH, mPFC *Adrb1* gene ($t = 4.621$, $P = 0.0099$, Fig. 1i) and ADRB1 protein ($t = 3.489$, $P = 0.0175$, Fig. 1j) were persistently at higher levels in METH-sired male mice (qPCR: $n = 3$ mice; protein: $n = 3$ mice) than that in SAL-sired male F1 (qPCR: $n = 3$ mice; protein: $n = 4$ mice).

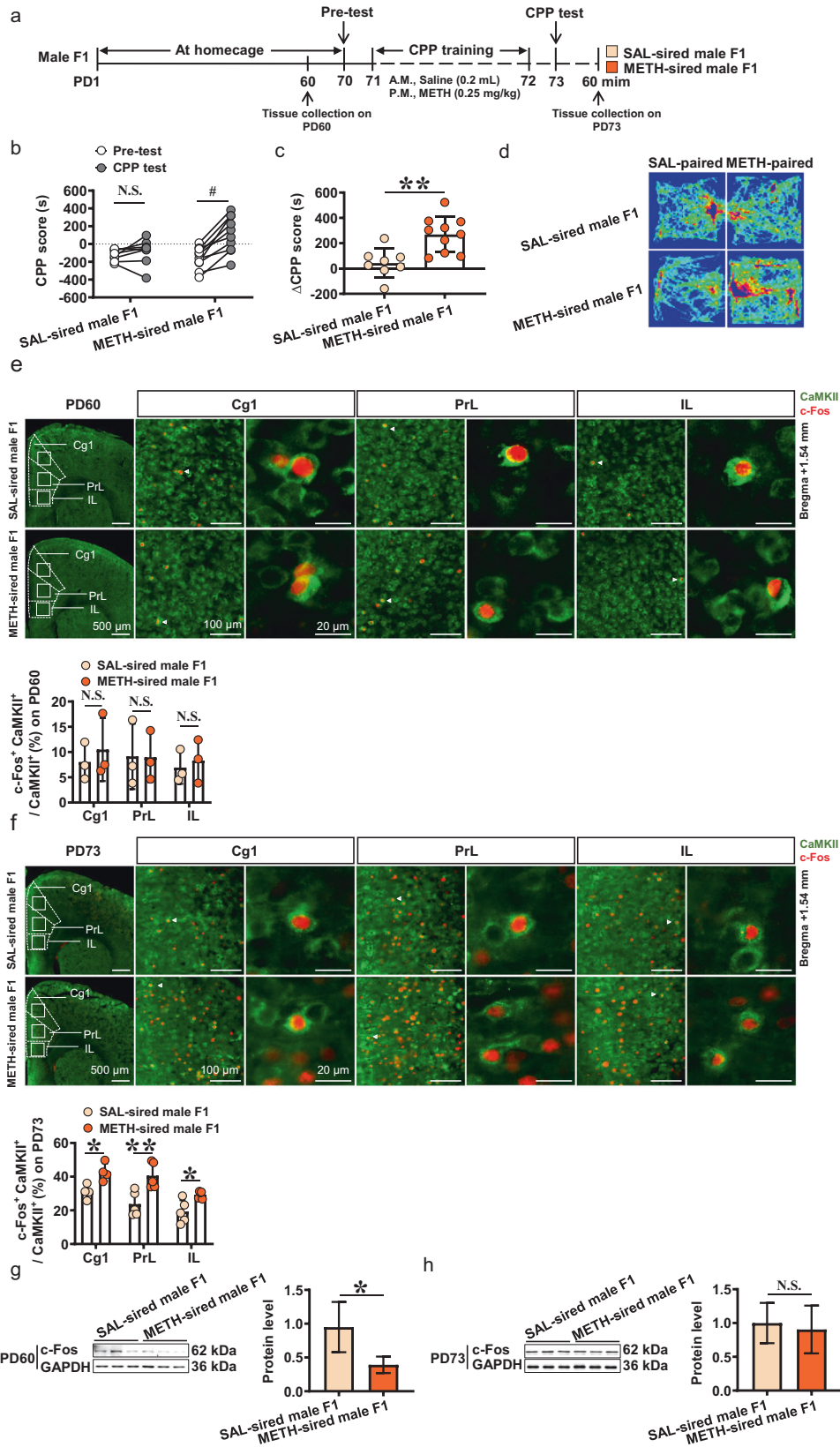
Further, ADRB1 levels on neurons of mPFC and its subregions (Fig. 1k–l) were examined by immunostaining. On PD60, the mean gray value of ADRB1 on neurons was much higher in the Cg1 ($t = 4.649$, $P = 0.0097$) and PrL ($t = 4.311$, $P = 0.0125$), and a high trend in IL ($t = 2.265$, $P = 0.0862$) of METH-sired male F1 ($n = 3$ mice) than that in SAL-sired male F1 ($n = 3$ mice). On PD73 following sd-METH, the mean gray value of ADRB1 on neurons was continuously higher in PrL ($t = 6.304$, $P = 0.0032$), and a higher trend in Cg1 ($t = 2.382$, $P = 0.0758$), IL ($t = 2.635$, $P = 0.0579$) of METH-sired male F1 ($n = 3$ mice), when compared to that in SAL-sired male F1 ($n = 3$ mice).

To observe the effects of sd-METH treatment on levels of *c-Fos* and ADRB1 on the mPFC under normal conditions, male naïve mice were subjected to subthreshold dose of METH treatment (Fig. S3a). Neither *c-Fos* gene ($t = 0.4522$, $P = 0.6745$, Fig. S3b) and *Adrb1* ($t = 0.9778$, $P = 0.3835$, Fig. S3b), nor *c-Fos* protein ($t = 1.115$, $P = 0.3274$, Fig. S3c) and ADRB1 protein ($t = 1.723$, $P = 0.1600$, Fig. S3c) in mPFC were changed by subthreshold dose of METH administration in naïve mice ($n = 3$ mice per group).

With these results, we infer that paternal METH exposure-increased ADRB1 on mPFC neurons might contribute to the higher sensitivity to METH in male F1 mice.

Blocking ADRB1 suppresses sd-METH-induced CPP in METH-sired male F1 mice

Here, betaxolol were bilaterally injected into mPFC (Fig. S4a) to block the activation of ADRB1. In Experiment 1 (Fig. 2a), a single dose of betaxolol were injected into mPFC at 15 min prior to sd-METH-induced CPP test. METH-sired male F1 did not exhibit METH-preferred behavior any more ($n = 8$ mice, $t = 1.666$, $P = 0.2219$), and METH-sired male F1 with vehicle treatment exhibited sd-METH-induced CPP continuously ($n = 8$ mice, $t = 3.518$, $P = 0.0068$). The Δ CPP score ($t = 3.666$, $P = 0.0025$) in



vehicle-injected METH-sired male F1 was much higher than that in betaxolol-injected METH-sired male F1 (Fig. 2b–d).

In Experiment 2 (Fig. 2e), betaxolol were bilaterally injected into mPFC during the whole period of CPP training. Betaxolol-treated

METH-sired male F1 mice did not acquire sd-METH-induced CPP ($n = 8$ mice, $t = 0.2852$, $P = 0.9514$), but vehicle-treated METH-sired male F1 mice still exhibit sd-METH-induced CPP ($n = 8$ mice, $t = 6.570$, $P < 0.0001$). The Δ CPP score ($t = 4.847$, $P = 0.0003$) in

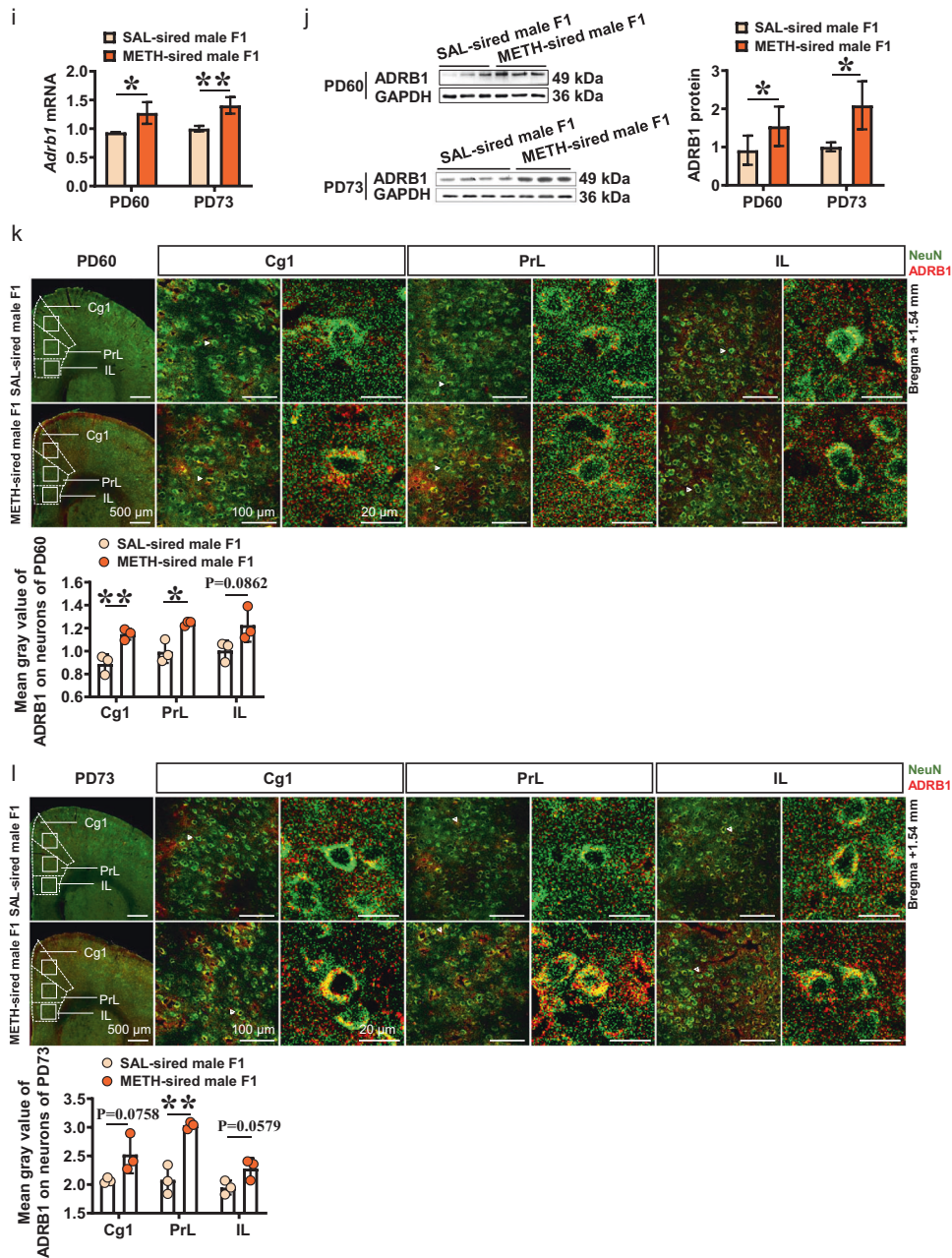


Fig. 1 The CPP, mPFC activity and ADRB1 level in male F1. **a** Experimental design and timeline. **b** CPP score by male F1. **c** Δ CPP score by male F1. **d** Traveled traces in CPP apparatus by male F1. **e, f** The percentage of c-Fos-positive cells in Cg1, PrL and IL on PD60 and on PD73. CaMKII and c-Fos were used as markers for the pyramidal neurons and activated neurons, respectively. Scale bar, 500 μ m /100 μ m /20 μ m. **g, h** Levels of c-Fos protein on PD60 and PD73. **i** Levels of *Adrb1* mRNA on PD60 and PD73. **j** Levels of ADRB1 protein on PD60 and PD73. **k, l** Mean gray value of ADRB1 on mPFC neurons on PD60 and PD73. Scale bar, 500 μ m /100 μ m /20 μ m. Cg1 cingulate cortex, PrL prelimbic cortex, IL infralimbic cortex. SAL-sired male F1, saline-sired male F1 mice; METH-sired male F1, methamphetamine-sired male F1 mice. The data are presented as the Mean \pm SD. Data were analyzed by two-way ANOVA followed by Sidak's multiple comparisons test where appropriate. N.S., $P > 0.05$. * $P < 0.05$ vs baseline (Pre-test CPP score). ** $P < 0.05$, *** $P < 0.01$ vs SAL-sired male F1.

vehicle-injected METH-sired male F1 was much higher than that in betaxolol-injected METH-sired male F1 (Fig. 2f–h).

Here, we also examine the effects of betaxolol on sd-METH-induced CPP in SAL-sired male F1 mice. In Experiment S1 (Fig. S4b–e), similar to the above results, sd-METH could not induce CPP in SAL-sired male F1 ($n = 5$ mice, $t = 0.1464$, $P = 0.9872$). Further, a single dose of betaxolol administration at 15 min prior to CPP did not affect their CPP score as well ($n = 6$ mice, $t = 0.1320$, $P = 0.9896$). There was no difference in the Δ CPP score ($t = 0.01917$, $P = 0.9851$) between vehicle-treated and betaxolol-treated SAL-sired male F1. In

Experiment S2 (Fig. S4f–i), similarly, sd-METH treatment could not induce CPP in SAL-sired male F1 ($n = 6$ mice, $t = 0.5901$, $P = 0.8136$). The betaxolol injection during CPP training did not significantly affect their CPP scores as well ($n = 6$ mice, $t = 0.4447$, $P = 0.8884$). There was no difference in the Δ CPP score ($t = 0.4406$, $P = 0.6689$) between vehicle-treated and betaxolol-treated SAL-sired male F1.

These results indicate that mPFC ADRB1 mediate both formation (CPP training) and expression (CPP test) of sd-METH-induced CPP in METH-sired F1 mice, and contribute to paternal METH exposure-increased sensitivity to METH in male F1 mice.

Knocking-down ADRB1^{CaMKII} blocks sd-METH-induced CPP in METH-sired male F1 mice

Here, adeno-associated virus (AAV) were used to knocking-down ADRB1 on CaMKII-positive neurons (ADRB1^{CaMKII}) within mPFC (Fig. 3a). As shown in Fig. 3b, AAV of *CaMKIIap-EGFP-MIR155(MCS)-SV40PolyA* (KD group) or AAV of *CaMKIIap-EGFP-SV40PolyA* (Ctrl group) were bilaterally infused into mPFC on P55, which could specifically transfect CaMKII-positive neurons. On P70, about 60%~80% CaMKII-positive neurons were transfected with virus (Fig. 3c). The levels of *Adrb1* gene ($t = 7.361$, $P = 0.0018$, Fig. 3d), ADRB1 protein ($t = 4.286$, $P = 0.0128$, Fig. 3e), and ADRB1^{CaMKII} expression ($t = 4.237$, $P = 0.0133$, Fig. 3f) were all reduced in mPFC of male F1 by KD virus ($n = 3$ mice), when compared with Ctrl virus ($n = 3$ mice), indicating good efficiency of KD virus.

As shown Fig. 3g-i, Ctrl virus-treated METH-sired male F1 mice still acquired sd-METH-induced CPP ($n = 12$ mice, $t = 8.228$, $P < 0.0001$), but KD virus-treated METH-sired male F1 mice did not exhibit METH-preferred behaviors and even produced METH-aversion behaviors ($n = 10$ mice, $t = 3.253$, $P = 0.008$), when compared with their corresponding Pre-test score. The Δ CPP score of KD group was much lower than that in Ctrl group ($t = 7.95$, $P < 0.0001$).

These results confirmed that mPFC ADRB1^{CaMKII} mediate paternal METH exposure-induced higher sensitivity to METH in male F1 mice.

Knocking-down ADRB1^{CaMKII} reduces mPFC activation in METH-sired male F1 mice

Compared to Ctrl group (protein, $n = 3$ mice; immunostaining, $n = 6$ mice; dendritic spine density, $n = 6$ mice), knocking-down mPFC ADRB1^{CaMKII} obviously decreased levels of c-Fos protein ($t = 5.372$, $P = 0.0058$, Fig. 4a) and immunostaining ($t = 3.136$, $P = 0.0106$, Fig. 4b), and dendritic spine density of CaMKII-positive neurons ($t = 3.891$, $P = 0.003$, Fig. 4c) in mPFC of METH-sired male F1 (protein, $n = 3$ mice; immunostaining, $n = 6$ mice; dendritic spine density, $n = 6$ mice).

The potential subsequent molecules of β -adrenergic signaling pathways especially β -arrestin2 and PKA, were examined in mPFC. Compared to Ctrl virus group ($n = 3-6$ mice), protein levels of β -arrestin2 ($t = 0.4597$, $P = 0.6555$) and PKA ($t = 0.6055$, $P = 0.5775$, Fig. 4d) were not changed, the p-ERK1/2 ($t = 8.202$, $P < 0.0001$), ratio of p-ERK1/2 to ERK1/2 ($t = 2.486$, $P = 0.0347$) and Δ FosB ($t = 2.944$, $P = 0.0147$) were decreased, and ERK1/2 ($t = 0.9153$, $P = 0.3839$), CREB ($t = 0.5454$, $P = 0.6145$), p-CREB ($t = 0.8085$, $P = 0.4641$) and ratio of p-CREB to CREB ($t = 0.6042$, $P = 0.5783$) were not changed in mPFC by knocking-down ADRB1 ($n = 3-6$ mice, Fig. 4e).

These results indicate that ADRB1^{CaMKII} positively activate mPFC CaMKII-positive neurons, and p-ERK1/2 and Δ FosB are the subsequent signals for ADRB1 in the process.

DISCUSSION

The current study found that paternal METH exposure induces higher ADRB1 levels on mPFC neurons. The subthreshold dose of METH (sd-METH), which is insufficient to produce CPP normally, efficiently induced METH-related CPP in METH-sired male F1, accompanied with more activated CaMKII-positive neurons and continuous higher ADRB1 in their mPFC. Either inhibiting ADRB1 function or knocking-down ADRB1 levels on CaMKII-positive neurons (ADRB1^{CaMKII}) could efficiently reduce sd-METH-evoked mPFC activation and block sd-METH-induced CPP in METH-sired male F1. These results indicate that paternal METH exposure induce a higher sensitivity to METH in male offspring potentially through driving mPFC ADRB1^{CaMKII} (Fig. 5).

METH is commonly abused psychostimulant among men of reproductive age. Consistent with previous studies, we found that sd-METH, which is insufficient to induce CPP in naïve mice,

effectively induced METH-preferred behaviors in METH-sired male F1 but not in METH-sired female F1, indicating paternal METH use affect susceptibility of F1 to drugs in a gender-dependent manner. Recently, a number of longitudinal studies indicate that there is a gender difference in the vulnerability to the toxicity of prenatal substance abuse in offspring [29–31]. Previously, using the same mice models, we found that METH-sired female F1 mice showed more anxiety-like behaviors and spatial memory deficit than those of male F1 [11]. Here, we found that METH-sired male F1 mice were much more vulnerability to drugs during adulthood than female F1. We believe that there are many factors contributing to these gender differences, which at least include: (1) Different metabolic profile in response to drugs between genders. Previously, we found that there is a significant difference in metabolomics of blood sample between male and female addicts, as showed more betaine, cortisol, 7,8-dihydrobiopterin and 4-hydroxybenzoic acid in females, and more L-phenylalanine, Ltryptophan, L-histidine, xanthosine, adenosine 5'-monophosphate in males [32], indicating different metabolic process in response to METH between males and females. (2) The influence of menstrual cycle in female should be taken into consideration. Recently, evidences suggest that estrogen could induce, while progesterin attenuate the formation of drug addiction in females [33, 34], implying the menstrual cycle might affect the susceptibility to drugs in females. Therefore, it should be further explored in the future study whether METH-sired female F1 mice would show different susceptibility to drugs at different phase of menstrual cycle. (3) The responsivity of brains to parental drug exposure in offspring with a gender-specific manner. As our previous study, male F1 mice has a different responsive pattern to paternal METH exposure, when compared to female F1 mice, including the mPFC and its subregions [11].

The mPFC has been implicated in the vulnerability to drug abuse [6–8]. Currently, little literature uncover the association of paternal METH intake with offspring mPFC alteration. *In utero* exposure to cocaine had been reported to increase the induction of long-term potentiation (LTP) and neuronal excitability at pyramidal neurons in mPFC of offspring [35], an increase in dendritic spines of II/III layer of pyramidal neurons in mPFC of offspring [36], and a reduction of the sensitivity of locomotor activity to cocaine in offspring rats [35, 37]. By contrast, Yan et al. [38] reported prenatal cocaine exposure attenuated baseline levels of mature BDNF protein in offspring brain, and Cantacorps et al. [39] found prenatal alcohol exposure increased vulnerability to cocaine addiction in adult mice via a greater glutamate receptor in mPFC. Similarly, human imaging studies demonstrated that prenatal cocaine exposed-adolescents exhibited less capability of increasing their PFC activation in response to memory load [40], and infants with prenatal cocaine use had a lesser gray matter in prefrontal brain regions [41, 42]. In addition, adolescents with prenatal cocaine exposure had reduced activity in PFC when exposing to favorite-food cues [43]. Although there are conflicting results among these studies, they suggest that plasticity of frontal brain play essential roles in prenatal drugs intake-elicited heritable susceptibility to addiction in offspring. Here, we found that paternal METH exposure seemed to reduce mPFC activity in male F1, as indicated by lower levels of c-Fos in mPFC. However, sd-METH treatment, which could not activate mPFC in naïve mice, reversely triggered mPFC activation in METH-sired male F1, implying potential intrinsic molecules in mPFC that may contribute to paternal METH exposure-increased sensitivity to METH in male F1 mice. How parental experiences of drug abuse being transmitted to offspring, causing brain changes, and subsequently leading to behavioral changes in offspring, remains unclear. Recently, many studies have explored the potential transgenerational mechanism from the perspective of germ cell, especially from the epigenetic perspectives. For example, sperm DNA methylation [44, 45] has been believed as an essential

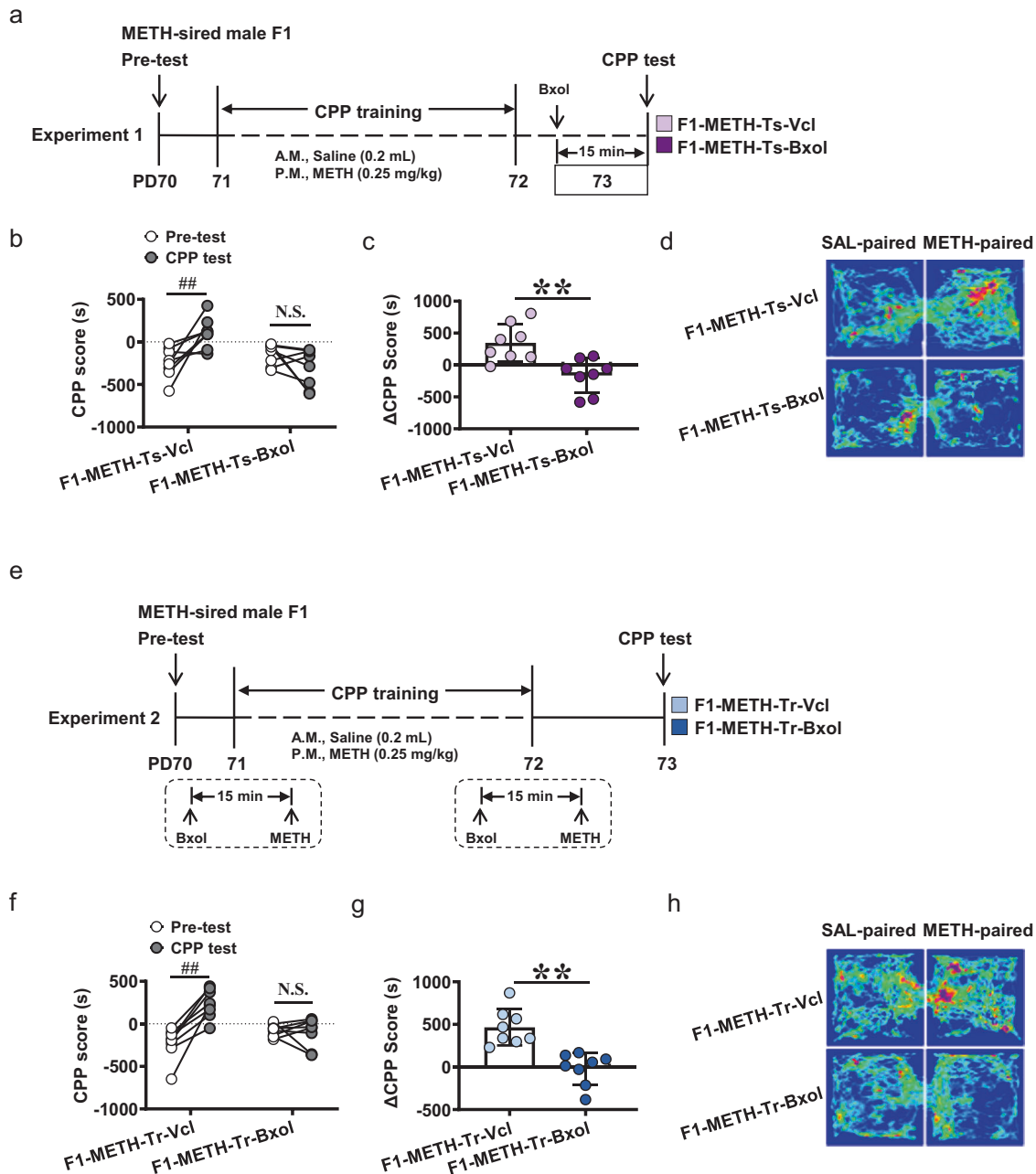


Fig. 2 Effects of betaxolol on *sd*-METH-induced CPP in METH-sired male F1. **a** Timeline of Experiment 1. **b** CPP score. **c** Δ CPP score. **d** Traveled traces in the CPP apparatus by METH-sired male F1. **e** Timeline of Experiment 2. **f** CPP score. **g** Δ CPP score. **h** Traveled traces in the CPP apparatus by METH-sired male F1. F1-METH-Ts-Vcl, vehicle bilaterally into the mPFC of METH-sired male F1 at 15 min prior to CPP test; F1-METH-Ts-Bxol, betaxolol bilaterally into the mPFC of METH-sired male F1 at 15 min prior to CPP test; F1-METH-Tr-Vcl, vehicle bilaterally into the mPFC of METH-sired male F1 during CPP training; F1-METH-Tr-Bxol, betaxolol bilaterally into the mPFC of METH-sired male F1 during CPP training. The data are presented as the Mean \pm SD. Data were analyzed by two-way ANOVA followed by Sidak's multiple comparisons test where appropriate. N.S., $P > 0.05$. ## $P < 0.01$ vs Pre-test CPP score. ** $P < 0.01$ vs F1-METH-Ts-Vcl or F1-METH-Tr-Vcl.

mechanism to transmit the environment-caused epigenetic alterations to progeny [46, 47], including its potential role in the susceptibility to the drugs in offspring prenatally exposed to cocaine [48] and METH [49, 50]. Compared to laboratory animals, the factors underlying transgenerational inheritance of addiction are far-more complicated in humans. One study reported that METH use had no obviously influence on sexual performance in male rats [51]. While, METH abuse related abnormal behaviors might transmit from one person to another (e.g., from father to mother) in humans, increasing the risk of experiencing emotional and psychological problems, even substance use in mother

[52–54], which may also contribute to the increased sensitivity to drugs in METH-sired offspring.

ADRB1 is highly expressed on glutamatergic neurons of mPFC. In general, endogenous activation of ADRB1 excites neurons via eliciting the depolarization on the membrane potential in mPFC [55]. An early study found that prenatal cocaine exposure increased cortical ADRB1 about 68% in pup rats at 30 days of age, a time when these rats showed hyperactivity [56]. Unfortunately, few studies further explored the role of this increase of cortical ADRB1 in addiction or related psychiatric disorders of offspring. Administration of betaxolol, a selective ADRB1

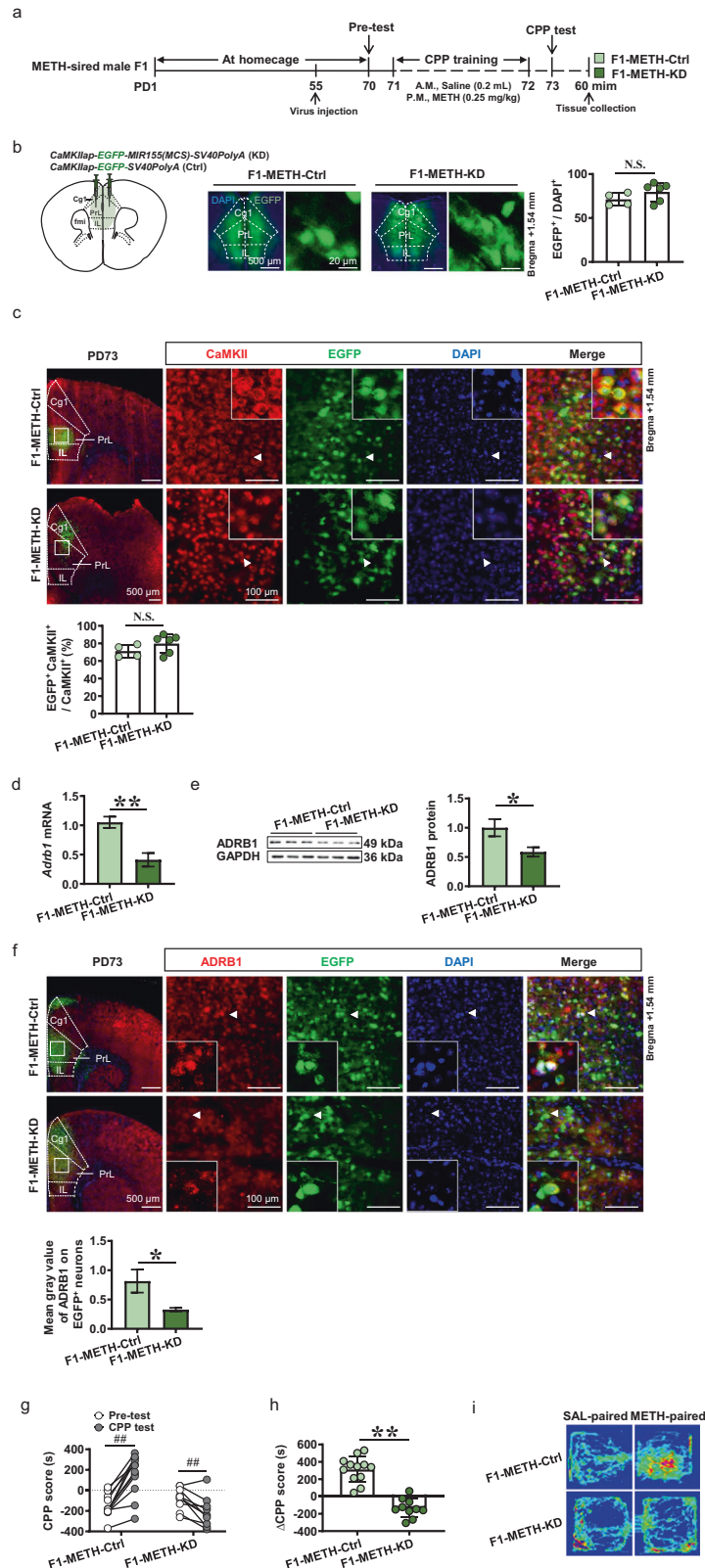


Fig. 3 Effects of knocking-down ADRB1^{CaMKII} on sd-METH-induced CPP in METH-sired male F1. **a** Experimental design and timeline. **b** Schematic diagram of viral injection and representative images of viral transfection in mPFC (middle panel). Scale bar, 500 μ m / 20 μ m. **c** Percentage of viral transfected neurons in the total pyramidal neurons of mPFC. Scale bar, 500 μ m / 100 μ m. **d** Levels of *Adrb1* mRNA in mPFC. **e** Levels of ADRB1 protein in mPFC. **f** Mean gray value of ADRB1 on virus transfected neurons of mPFC. Scale bar, 500 μ m / 100 μ m. **g** CPP score. **h** Δ CPP score. **i** Traveled traces in the CPP apparatus by METH-sired male mice. F1-METH-Ctrl, METH-sired male F1 mice injected with Ctrl virus. F1-METH-KD, METH-sired male F1 mice injected with KD virus. The data are presented as the Mean \pm SD. Data were analyzed by two-way ANOVA followed by Sidak's multiple comparisons test where appropriate. N.S., $P > 0.05$. ## $P < 0.01$ vs pre-test CPP score. * $P < 0.05$, ** $P < 0.01$ vs F1-METH-Ctrl.

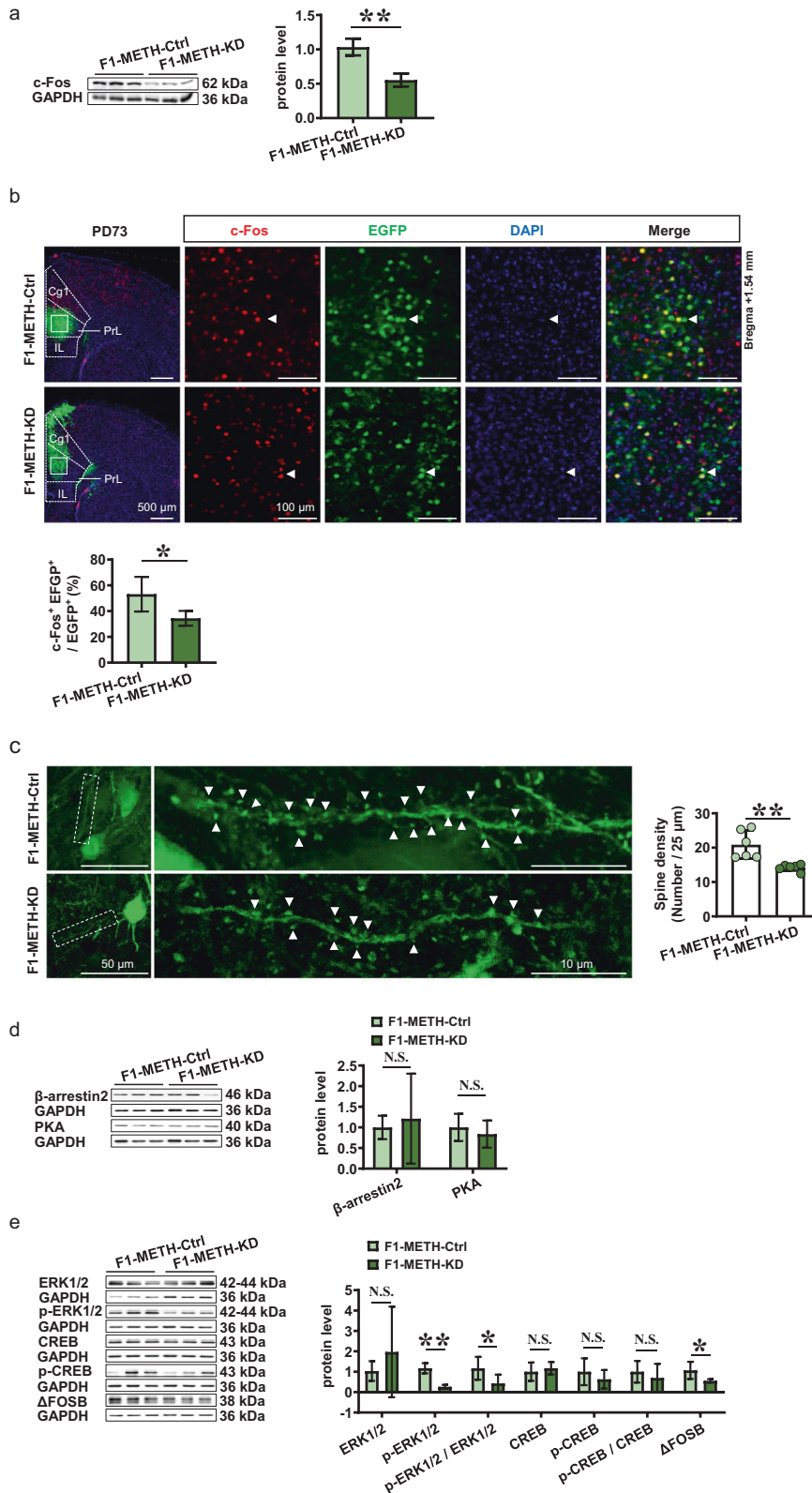


Fig. 4 Effects of knocking-down ADRB1^{CaMKII} on mPFC activity and subsequent signals in METH-sired male F1. **a** Levels of c-Fos protein. **b** The c-Fos immunostaining. Scale bar, 500 μm /100 μm. **c** Density of dendritic spine. Scale bar, 50 μm /10 μm. **d** Levels of β-arrestin2 and PKA protein. **e** Levels of ERK1/2, p-ERK1/2, ERK1/2/p-ERK1/2, CREB, p-CREB, p-CREB/ CREB and ΔFosB protein. F1-METH-Ctrl, METH-sired male F1 mice injected with Ctrl virus. F1-METH-KD, METH-sired male F1 mice injected with KD virus. The data are presented as the Mean ± SD. N.S., $P > 0.05$. * $P < 0.05$, ** $P < 0.01$ vs F1-METH-Ctrl.

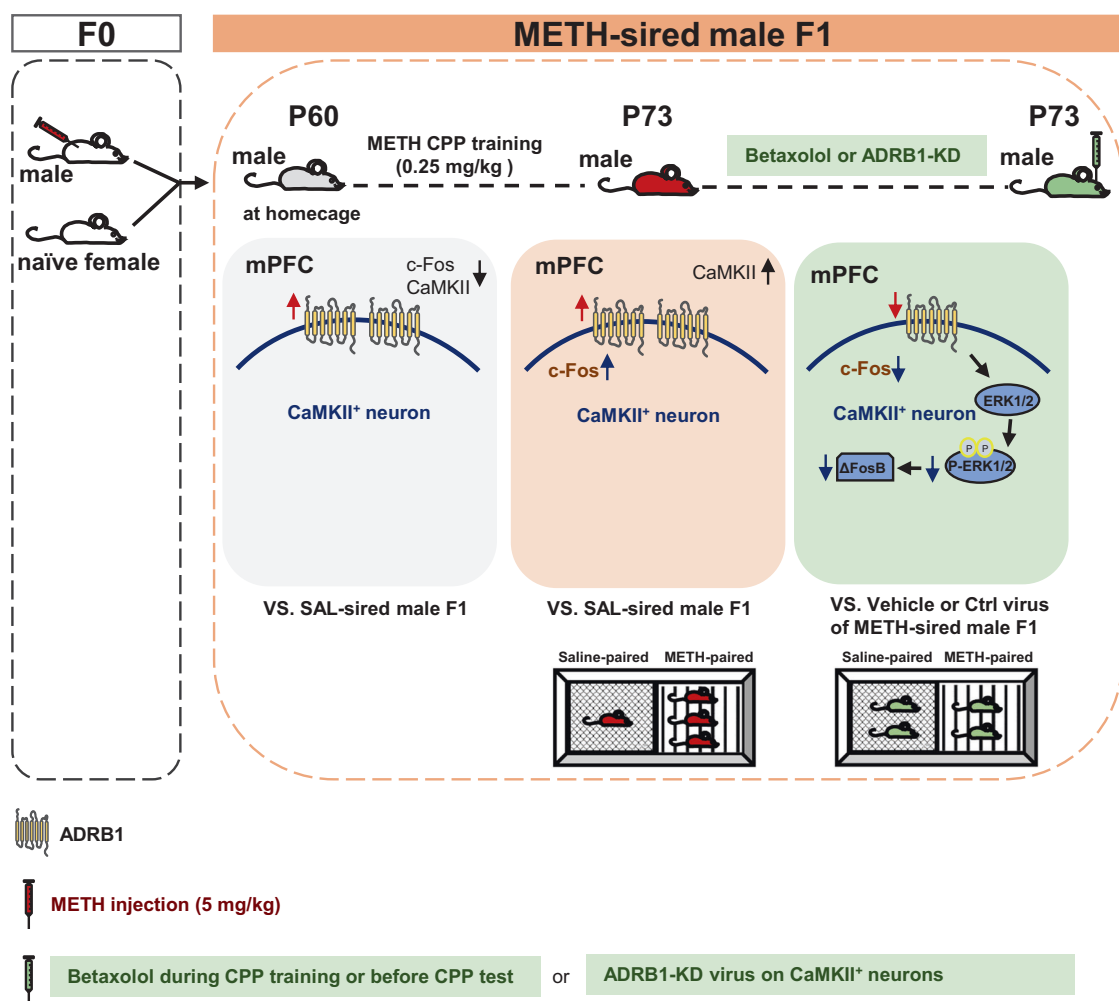


Fig. 5 Schematic summary of this study. Paternal methamphetamine (METH) exposure induces higher ADRB1 levels on mPFC neurons in male F1 mice during adulthood. Subthreshold dose of METH treatment in F1 (sd-METH), which is not sufficient to induce CPP, efficiently produces METH-related CPP in METH-sired male F1 mice, accompanied with more activated mPFC CaMKII-positive neurons than that in saline-sired male F1 mice. Locally inhibiting ADRB1 function or specifically knocking-down ADRB1 on CaMKII-positive neurons (ADRB1^{CaMKII}) efficiently reduces sd-METH-evoked mPFC activation, and ultimately blocks sd-METH-induced CPP in METH-sired male F1 mice. The p-ERK1/2 and ΔFosB might be potential subsequent signals of ADRB1 in the process.

antagonist, blocked reinstatement of cocaine CPP [19]. Further, blocking ADRB1 impaired reconsolidation and reinstatement of cocaine self-administration [57]. Here, we found that paternal METH exposure increased ADRB1 on mPFC neurons. We believe that this higher ADRB1 is kind of compensatory effect for brain injury in offspring of sires exposed to drugs, which could strengthen the sensitivity of neurons to internal or external stimuli. Following sd-METH treatment, we observed a continuous higher ADRB1 level in METH-sired male F1. Blocking ADRB1 or knocking-down ADRB1 on CaMKII-positive neurons (ADRB1^{CaMKII}) efficiently reduced sd-METH-evoked mPFC activation, and ultimately blocked sd-METH-induced CPP in METH-sired male F1. These results indicate that ADRB1^{CaMKII} mediate mPFC activity, which is one key intrinsic molecule of mPFC for the paternal METH exposure-induced higher sensitivity in male offspring. There is a query that whether the ADRB1 changes in METH-sired F1 are specific to rewarding circuitry. Previously, we found that METH-sired F1 mice exhibited more anxiety-like behaviors and spatial memory deficits [11], and paternal cocaine experience increased anxiety-like behaviors [58] and memory formation deficits [59] in offspring. We believed that these abnormal behaviors caused by paternal drug use should be interact with each other, and share common brain mechanisms. Thus, we would investigate the role

of ADRB1 in different brain regions besides rewarding circuitry and other kinds of abnormal behaviors in offspring prenatally exposed to drugs.

ADRB1 activates neurons by eliciting its downstream protein kinases and signal pathways (e.g. PKA, β-arrestin2), or mediating the function of nearby channels (e.g. TREK-2-like channels) or receptors (e.g. GluR1) on the membrane of cells. The critical role of ADRB1/cyclic-AMP dependent PKA in synaptic plasticity of the frontal cortex are well-studied [60]. Recently, Huang et al. found that ADRB1/β-arrestin/ERK signaling in entorhinal cortex, acting as a non-classical G protein-coupled pathway, mediated memory reconsolidation [28]. Their lab later reported that overexpression of β-arrestin2 in PFC promoted extinction learning of cocaine-induced CPP, which was blocked by propranolol, a nonbiased β-adrenergic receptor antagonist [61]. Thus, we detected the molecules related to ADRB1, especially those of β-arrestin2-dependent and PKA-dependent signal proteins. Unexpected, the levels of β-arrestin2 and PKA failed to change in mPFC after knocking-down ADRB1. While, we found that knocking-down ADRB1 effectively reduce the levels of p-ERK1/2 and ΔFosB in mPFC. Son et al. [62] has been reported that acupuncture exert its therapeutic effects on METH-induced addiction via suppression of METH-increased p-ERK1/2 and ΔFosB in PFC. The p-ERK1/

2 signaling cascades in PFC has been thought of important contributor for the development of METH addiction [63]. Δ FosB, a transcription factor, is increased in PFC by drugs including METH [62] and Δ 9-tetrahydrocannabinol (THC) [64], which leads to a long-lasting enhanced behavioral response. Further, Δ FosB is preferentially induced by cocaine in adolescent animals, which engaged in the higher vulnerability to addiction [65]. Unlike c-Fos, Arc and ERK, Δ FosB maintains adaptive changes in brain for a long time following drugs of abuse [66], which is involved in the long-term pathological plasticity of brain and persistent addictive behavior by drugs [67]. Together with our present study, these findings revealed that p-ERK1/2 and Δ FosB may be subsequent signals for ADRB1 mediating heritable susceptibility to addiction in offspring.

Currently, the agonists and antagonists of ADRB1 has not been approached in clinical treatment for addiction and related psychiatric comorbidity. Vranjkovic et al. [19] reported that targeting β -adrenergic receptors, including ADRB1, might represent a promising pharmacotherapeutic strategy for preventing drug relapse, particularly being induced by stress in cocaine addicts. Together with our finding that mPFC ADRB1^{CaMKII} is involved in increased sensitivity to drug in METH-sired male F1 mice, therefore ADRB1 might be considered as a potential target for predicting and treating the transgenerational susceptibility to addiction caused by paternal drug exposure.

DATA AVAILABILITY

The data that support the findings of this study are available from the corresponding author upon reasonable request.

REFERENCES

- Verstegen RHJ, Wang G, Langenberg-Verbergaert KPS, Ren LY, Nulman I. Paternal exposure to recreational drugs before conception and its effect on live-born offspring: a scoping review. *Birth Defects Res.* 2020;112:970–88.
- Goldberg LR, Gould TJ. Multigenerational and transgenerational effects of paternal exposure to drugs of abuse on behavioral and neural function. *Euro J Neurosci.* 2019;50:2453–66.
- Mihalčíková L, Ochozková A, Šlamberová R. Does paternal methamphetamine exposure affect the behavior of rat offspring during development and in adulthood? *Physiol Res.* 2021;70:5419–530.
- Cordie R, McFadden LM. Optogenetic inhibition of the medial prefrontal cortex reduces methamphetamine-primed reinstatement in male and female rats. *Behav Pharmacol.* 2019;30:506–13.
- Parsegian A, See RE. Dysregulation of dopamine and glutamate release in the prefrontal cortex and nucleus accumbens following methamphetamine self-administration and during reinstatement in rats. *Neuropsychopharmacol Off Publ Am Coll Neuropsychopharmacol.* 2014;39:811–22.
- Perry JL, Joseph JE, Jiang Y, Zimmerman RS, Kelly TH, Darna M, et al. Prefrontal cortex and drug abuse vulnerability: translation to prevention and treatment interventions. *Brain Res Rev.* 2011;65:124–49.
- Li H, Chen J-A, Ding Q-Z, Lu G-Y, Wu N, Su R-B, et al. Behavioral sensitization induced by methamphetamine causes differential alterations in gene expression and histone acetylation of the prefrontal cortex in rats. *BMC Neurosci.* 2021;22:24.
- Goldstein RZ, Volkow ND. Dysfunction of the prefrontal cortex in addiction: neuroimaging findings and clinical implications. *Nat Rev Neurosci.* 2011;12:652–69.
- González B, Jayanthi S, Gomez N, Torres OV, Sosa MH, Bernardi A, et al. Repeated methamphetamine and modafinil induce differential cognitive effects and specific histone acetylation and DNA methylation profiles in the mouse medial prefrontal cortex. *Progress Neuro-Psychopharmacol Biol Psychiatry.* 2018;82:1–11.
- Haddar M, Uno K, Azuma K, Muramatsu S-I, Nitta A. Inhibitory effects of Shati/Nat8l overexpression in the medial prefrontal cortex on methamphetamine-induced conditioned place preference in mice. *Addiction Biol.* 2020;25:e12749.
- Fan Y, Li Z, Zheng Y, Wei X, Zhang Z, Cai Q, et al. Sex-specific neurobehavioural outcomes and brain stimulation pattern in adult offspring paternally exposed to methamphetamine. *Addiction Biol.* 2022;27:e13175.
- Coutellier L, Ardestani PM, Shamloo M. β 1-adrenergic receptor activation enhances memory in Alzheimer's disease model. *Ann Clin Transl Neurol.* 2014;1:348–60.
- Goodman AM, Langner BM, Jackson N, Alex C, McMahon LL. Heightened hippocampal β -adrenergic receptor function drives synaptic potentiation and supports learning and memory in the TgF344-AD rat model during prodromal Alzheimer's disease. *J Neurosci Off J Soc Neurosci.* 2021;41:5747–61.
- Rudoy CA, Reyes A-RS, Van Bockstaele EJ. Evidence for beta1-adrenergic receptor involvement in amygdalar corticotropin-releasing factor gene expression: implications for cocaine withdrawal. *Neuropsychopharmacol Off Publ Am Coll Neuropsychopharmacol.* 2009;34:1135–48.
- Sun Q, Huang J, Yang DL, Cao XN, Zhou WL. Activation of β -adrenergic receptors during sexual arousal facilitates vaginal lubrication by regulating vaginal epithelial Cl(-) secretion. *J Sexual Med.* 2014;11:1936–48.
- You Z-B, Galaj E, Alén F, Wang B, Bi G-H, Moore AR, et al. Involvement of the ghrelin system in the maintenance and reinstatement of cocaine-motivated behaviors: a role of adrenergic action at peripheral β 1 receptors. *Neuropsychopharmacol Off Publ Am Coll Neuropsychopharmacol.* 2022;47:1449–60.
- Sugama S, Takenouchi T, Hashimoto M, Ohata H, Takenaka Y, Kakinuma Y. Stress-induced microglial activation occurs through β -adrenergic receptor: noradrenaline as a key neurotransmitter in microglial activation. *J Neuroinflammation.* 2019;16:266.
- Ji X-H, Cao X-H, Zhang C-L, Feng Z-J, Zhang X-H, Ma L, et al. Pre- and postsynaptic β -Adrenergic activation enhances excitatory synaptic transmission in layer V/VI pyramidal neurons of the medial prefrontal cortex of rats. *Cerebral Cortex.* 2007;18:1506–20.
- Vranjkovic O, Hang S, Baker DA, Mantsch JR. β -adrenergic receptor mediation of stress-induced reinstatement of extinguished cocaine-induced conditioned place preference in mice: roles for β 1 and β 2 adrenergic receptors. *J Pharmacol Exp Ther.* 2012;342:541–51.
- Hernández A, Burgos H, Mondaca M, Barra R, Núñez H, Pérez H, et al. Effect of prenatal protein malnutrition on long-term potentiation and BDNF protein expression in the rat entorhinal cortex after neocortical and hippocampal tetanization. *Neural Plasticity.* 2008;2008:646919.
- Thompson BL, Levitt P, Stanwood GD. Prenatal exposure to drugs: effects on brain development and implications for policy and education. *Nat Rev Neurosci.* 2009;10:303–12.
- Huang C-C, Liang Y-C, Hsu K-S. Prenatal cocaine exposure enhances long-term potentiation induction in rat medial prefrontal cortex. *Int J Neuropsychopharmacol.* 2011;14:431–43.
- Kalpachidou T, Raftogianni A, Melissa P, Kollia AM, Stylianopoulou F, Stamatakis A. Effects of a neonatal experience involving reward through maternal contact on the noradrenergic system of the rat prefrontal cortex. *Cereb Cortex.* 2016;26:3866–77.
- Meitzen J, Luoma JI, Stern CM, Mermelstein PG. β 1-Adrenergic receptors activate two distinct signaling pathways in striatal neurons. *J Neurochem.* 2011;116:984–95.
- Shenoy SK, Drake MT, Nelson CD, Houtz DA, Xiao K, Madabushi S, et al. beta-arrestin-dependent, G protein-independent ERK1/2 activation by the beta2 adrenergic receptor. *J Biol Chem.* 2006;281:1261–73.
- Wang J, Gareri C, Rockman HA. G-protein-coupled receptors in heart disease. *Circ Res.* 2018;123:716–35.
- Tilley DG. G protein-dependent and G protein-independent signaling pathways and their impact on cardiac function. *Circ Res.* 2011;109:217–30.
- Huang B, Li Y, Cheng D, He G, Liu X, Ma L. β -Arrestin-biased β -adrenergic signaling promotes extinction learning of cocaine reward memory. *Sci Signal.* 2018;11:eaam5402.
- Traccis F, Frau R, Melis M. Gender differences in the outcome of offspring prenatally exposed to drugs of abuse. *Front Behav Neurosci.* 2020;14:72.
- Konijnenberg C. Methodological issues in assessing the impact of prenatal drug exposure. *Substance Abuse: Res Treat.* 2015;9:39–44.
- LaGasse LL, Woules T, Newman E, Smith LM, Shah RZ, Derauf C, et al. Prenatal methamphetamine exposure and neonatal neurobehavioral outcome in the USA and New Zealand. *Neurotoxicol Teratol.* 2011;33:166–75.
- Cheng Z, Peng Y, Wen X, Chen W, Pan W, Xu X, et al. Sex-specific metabolic signatures in methamphetamine addicts. *Addiction Biol.* 2023;28:e13255.
- Kokane SS, Perrotti LI. Sex differences and the role of estradiol in mesolimbic reward circuits and vulnerability to cocaine and opiate addiction. *Front Behav Neurosci.* 2020;14:74.
- Moran-Santa Maria MM, Flanagan J, Brady K. Ovarian hormones and drug abuse. *Curr Psychiatry Rep.* 2014;16:511.
- Lu H, Lim B, Poo M-M. Cocaine exposure in utero alters synaptic plasticity in the medial prefrontal cortex of postnatal rats. *J Neurosci Off J Soc Neurosci.* 2009;29:12664–74.
- Morrow BA, Hajszan T, Leranath C, Elsworth JD, Roth RH. Prenatal exposure to cocaine is associated with increased number of spine synapses in rat prelimbic cortex. *Synapse.* 2007;61:862–5.

37. Crozatier C, Guerriero RM, Mathieu F, Giros B, Nosten-Bertrand M, Kosofsky BE. Altered cocaine-induced behavioral sensitization in adult mice exposed to cocaine in utero. *Brain Res Dev Brain Res*. 2003;147:97–105.
38. Yan QS, Zheng SZ, Yan SE. Prenatal cocaine exposure decreases brain-derived neurotrophic factor proteins in the rat brain. *Brain Res*. 2004;1009:228–33.
39. Cantacorps L, Montagud-Romero S, Luján M, Valverde O. Prenatal and postnatal alcohol exposure increases vulnerability to cocaine addiction in adult mice. *Br J Pharmacol*. 2020;177:1090–105.
40. Li Z, Santhanam P, Coles CD, Ellen Lynch M, Hamann S, Peltier S, et al. Prenatal cocaine exposure alters functional activation in the ventral prefrontal cortex and its structural connectivity with the amygdala. *Psychiatry Res*. 2013;213:47–55.
41. Rando K, Chaplin TM, Potenza MN, Mayes L, Sinha R. Prenatal cocaine exposure and gray matter volume in adolescent boys and girls: relationship to substance use initiation. *Biol Psychiatry*. 2013;74:482–9.
42. Grewen K, Burchinal M, Vachet C, Gouttard S, Gilmore JH, Lin W, et al. Prenatal cocaine effects on brain structure in early infancy. *NeuroImage*. 2014;101:114–23.
43. Yip SW, Lacadie CM, Sinha R, Mayes LC, Potenza MN. Prenatal cocaine exposure, illicit-substance use and stress and craving processes during adolescence. *Drug Alcohol Dependence*. 2016;158:76–85.
44. Vassoler FM, Sadri-Vakili G. Mechanisms of transgenerational inheritance of addictive-like behaviors. *Neuroscience*. 2014;264:198–206.
45. Stewart KR, Veselovska L, Kelsey G. Establishment and functions of DNA methylation in the germline. *Epigenomics*. 2016;8:1399–413.
46. Skinner MK. Role of epigenetics in developmental biology and transgenerational inheritance. *Birth Defects Res C Embryo Today*. 2011;93:51–5.
47. Breton CV, Landon R, Kahn LG, Enlow MB, Peterson AK, Bastain T, et al. Exploring the evidence for epigenetic regulation of environmental influences on child health across generations. *Commun Biol*. 2021;4:769.
48. Le Q, Yan B, Yu X, Li Y, Song H, Zhu H, et al. Drug-seeking motivation level in male rats determines offspring susceptibility or resistance to cocaine-seeking behaviour. *Nat Commun*. 2017;8:15527.
49. Numachi Y, Shen H, Yoshida S, Fujiyama K, Toda S, Matsuoka H, et al. Methamphetamine alters expression of DNA methyltransferase 1 mRNA in rat brain. *Neurosci Lett*. 2007;414:213–7.
50. Cheng M-C, Hsu S-H, Chen C-H. Chronic methamphetamine treatment reduces the expression of synaptic plasticity genes and changes their DNA methylation status in the mouse brain. *Brain Res*. 2015;1629:126–34.
51. Mihačičková L, Ochozková A, Šlamberová R. Effect of methamphetamine exposure on sexual behavior and locomotor activity of adult male rats. *Physiol Res*. 2019;68:5339–546.
52. Li JH, Liu JL, Zhang KK, Chen LJ, Xu JT, Xie XL. The adverse effects of prenatal METH exposure on the offspring: a review. *Front Pharmacol*. 2021;12:715176.
53. Sample SJ, Strathdee SA, Zians J, Patterson TL. Methamphetamine-using parents: the relationship between parental role strain and depressive symptoms. *J Stud Alcohol Drugs*. 2011;72:954–64.
54. Liles BD, Newman E, Lagasse LL, Derauf C, Shah R, Smith LM, et al. Perceived child behavior problems, parenting stress, and maternal depressive symptoms among prenatal methamphetamine users. *Child Psychiatry Hum Dev*. 2012;43:943–57.
55. Grzelka K, Kurowski P, Gawlak M, Szulczyk P. Noradrenaline modulates the membrane potential and holding current of medial prefrontal cortex pyramidal neurons via $\beta(1)$ -adrenergic receptors and HCN channels. *Front Cell Neurosci*. 2017;11:341.
56. Henderson MG, McConaughy MM, McMillen BA. Long-term consequences of prenatal exposure to cocaine or related drugs: effects on rat brain monoaminergic receptors. *Brain Res Bull*. 1991;26:941–5.
57. Zhu H, Zhou Y, Liu Z, Chen X, Li Y, Liu X, et al. $\beta 1$ -Adrenoceptor in the central amygdala is required for unconditioned stimulus-induced drug memory reconsolidation. *Int J Neuropsychopharmacol*. 2018;21:267–80.
58. White SL, Vassoler FM, Schmidt HD, Pierce RC, Wimmer ME. Enhanced anxiety in the male offspring of sires that self-administered cocaine. *Addiction Biol*. 2016;21:802–10.
59. Wimmer ME, Briand LA, Fant B, Guercio LA, Arreola AC, Schmidt HD, et al. Paternal cocaine taking elicits epigenetic remodeling and memory deficits in male progeny. *Mol Psychiatry*. 2017;22:1641–50.
60. Flores O, Pérez H, Valladares L, Morgan C, Gatica A, Burgos H, et al. Hidden prenatal malnutrition in the rat: role of β_1 -adrenoceptors on synaptic plasticity in the frontal cortex. *J Neurochem*. 2011;119:314–23.
61. Liu X, Ma L, Li HH, Huang B, Li YX, Tao YZ, et al. β -Arrestin-biased signaling mediates memory reconsolidation. *Proc Natl Acad Sci U.S.A.* 2015;112:4483–8.
62. Son JS, Jeong YC, Kwon YB. Regulatory effect of bee venom on methamphetamine-induced cellular activities in prefrontal cortex and nucleus accumbens in mice. *Biol Pharmaceutical Bull*. 2015;38:48–52.
63. Sun WL, Quizon PM, Zhu J. Molecular mechanism: ERK signaling, drug addiction, and behavioral effects. *Prog Mol Biol Transl Sci*. 2016;137:1–40.
64. Lazenka MF, Kang M, De DD, Selley DE, Sim-Selley LJ. $\Delta 9$ -tetrahydrocannabinol experience influences Δ FosB and downstream gene expression in prefrontal cortex. *Cannabis Cannabinoid Res*. 2017;2:224–34.
65. Ehrlich ME, Sommer J, Canas E, Unterwald EM. Periadolescent mice show enhanced DeltaFosB upregulation in response to cocaine and amphetamine. *J Neurosci Off J Soc Neurosci*. 2002;22:9155–9.
66. Perrotti LI, Weaver RR, Robison B, Renthal W, Maze I, Yazdani S, et al. Distinct patterns of DeltaFosB induction in brain by drugs of abuse. *Synapse*. 2008;62:358–69.
67. Nestler EJ, Barrot M, Self DW. DeltaFosB: a sustained molecular switch for addiction. *Proc Natl Acad Sci U.S.A.* 2001;98:11042–6.

AUTHOR CONTRIBUTIONS

ZY and LD have equal contribution to the manuscript. ZY, LD and LZ performed behavioral tests, morphological tests. GH, CW and LZ performed molecular experiments. HT, ZY, LX, FY carried out the virus-related experiment. FY and LD performed data analysis. ZZ, CQ and GF assist the data analysis. GX and FY wrote the manuscript. LD help to support the proposal. GX developed the overall concept.

FUNDING

This work is supported by National Natural Science Foundation of China (82271531 and 82071495), Natural Science Foundation of Jiangsu Province, China (BK20201398) and Natural Science Foundation of the Higher Education Institutions of Jiangsu Province, China (21KJB360007).

COMPETING INTERESTS

The authors declare no competing interests.


ADDITIONAL INFORMATION

Supplementary information The online version contains supplementary material available at <https://doi.org/10.1038/s41398-023-02624-x>.

Correspondence and requests for materials should be addressed to Yu Fan or Xiaowei Guan.

Reprints and permission information is available at <http://www.nature.com/reprints>

Publisher's note Springer Nature remains neutral with regard to jurisdictional claims in published maps and institutional affiliations.

 **Open Access** This article is licensed under a Creative Commons Attribution 4.0 International License, which permits use, sharing, adaptation, distribution and reproduction in any medium or format, as long as you give appropriate credit to the original author(s) and the source, provide a link to the Creative Commons license, and indicate if changes were made. The images or other third party material in this article are included in the article's Creative Commons license, unless indicated otherwise in a credit line to the material. If material is not included in the article's Creative Commons license and your intended use is not permitted by statutory regulation or exceeds the permitted use, you will need to obtain permission directly from the copyright holder. To view a copy of this license, visit <http://creativecommons.org/licenses/by/4.0/>.

© The Author(s) 2023